AMERICAN SOCIETY FOR MICROBIOLOGY | Applied and Environmental Microbiology®

GEOMICROBIOLOGY

Nitrate Removal by a Novel Lithoautotrophic Nitrate-Reducing, Iron(II)-Oxidizing Culture Enriched from a Pyrite-Rich Limestone Aquifer

Natalia Jakus,[a,b] Nia Blackwell,[b] Karsten Osenbrück,[c] Daniel Straub,[b,d] James M. Byrne,[a] Zhe Wang,[e] David Glöckler,[f] Martin Elsner,[f] Tillmann Lueders,[e] Peter Grathwohl,[c] Sara Kleindienst,[b] Andreas Kappler[a,g]

[a]Geomicrobiology, Center for Applied Geoscience, University of Tuebingen, Tuebingen, Germany
[b]Microbial Ecology, Center for Applied Geoscience, University of Tuebingen, Tuebingen, Germany
[c]Hydrogeochemistry, Center for Applied Geoscience, University of Tuebingen, Tuebingen, Germany
[d]Quantitative Biology Center (QBiC), University of Tuebingen, Tuebingen, Germany
[e]Chair of Ecological Microbiology, Bayreuth Center of Ecology and Environmental Research (BayCEER), University of Bayreuth, Bayreuth, Germany
[f]Analytical Chemistry and Water Chemistry, Technical University of Munich, Munich, Germany
[g]Cluster of Excellence, EXC 2124, Controlling Microbes to Fight Infection, Tübingen, Germany

ABSTRACT Nitrate removal in oligotrophic environments is often limited by the availability of suitable organic electron donors. Chemolithoautotrophic bacteria may play a key role in denitrification in aquifers depleted in organic carbon. Under anoxic and circumneutral pH conditions, iron(II) was hypothesized to serve as an electron donor for microbially mediated nitrate reduction by Fe(II)-oxidizing (NRFeOx) microorganisms. However, lithoautotrophic NRFeOx cultures have never been enriched from any aquifer, and as such, there are no model cultures available to study the physiology and geochemistry of this potentially environmentally relevant process. Using iron(II) as an electron donor, we enriched a lithoautotrophic NRFeOx culture from nitrate-containing groundwater of a pyrite-rich limestone aquifer. In the enriched NRFeOx culture that does not require additional organic cosubstrates for growth, within 7 to 11 days, 0.3 to 0.5 mM nitrate was reduced and 1.3 to 2 mM iron(II) was oxidized, leading to a stoichiometric NO_3^-/Fe(II) ratio of 0.2, with N_2 and N_2O identified as the main nitrate reduction products. Short-range ordered Fe(III) (oxyhydr)oxides were the product of iron(II) oxidation. Microorganisms were observed to be closely associated with formed minerals, but only few cells were encrusted, suggesting that most of the bacteria were able to avoid mineral precipitation at their surface. Analysis of the microbial community by long-read 16S rRNA gene sequencing revealed that the culture is dominated by members of the *Gallionellaceae* family that are known as autotrophic, neutrophilic, and microaerophilic iron(II) oxidizers. In summary, our study suggests that NRFeOx mediated by lithoautotrophic bacteria can lead to nitrate removal in anthropogenically affected aquifers.

IMPORTANCE Removal of nitrate by microbial denitrification in groundwater is often limited by low concentrations of organic carbon. In these carbon-poor ecosystems, nitrate-reducing bacteria that can use inorganic compounds such as Fe(II) (NRFeOx) as electron donors could play a major role in nitrate removal. However, no lithoautotrophic NRFeOx culture has been successfully isolated or enriched from this type of environment, and as such, there are no model cultures available to study the rate-limiting factors of this potentially important process. Here, we present the physiology and microbial community composition of a novel lithoautotrophic NRFeOx culture enriched from a fractured aquifer in southern Germany. The culture is dominated by a putative Fe(II) oxidizer affiliated with the *Gallionellaceae* family and performs nitrate reduction coupled to Fe(II) oxidation leading to N_2O and N_2 formation without the addition of

Citation Jakus N, Blackwell N, Osenbrück K, Straub D, Byrne JM, Wang Z, Glöckler D, Elsner M, Lueders T, Grathwohl P, Kleindienst S, Kappler A. 2021. Nitrate removal by a novel lithoautotrophic nitrate-reducing, iron(II)-oxidizing culture enriched from a pyrite-rich limestone aquifer. Appl Environ Microbiol 87:e00460-21. https://doi.org/10.1128/AEM.00460-21.

Editor Alfons J. M. Stams, Wageningen University

Address correspondence to Andreas Kappler, andreas.kappler@uni-tuebingen.de.

Received 5 March 2021
Accepted 25 May 2021
Accepted manuscript posted online 4 June 2021
Published 27 July 2021

organic substrates. Our analyses demonstrate that lithoautotrophic NRFeOx can potentially lead to nitrate removal in nitrate-contaminated aquifers.

KEYWORDS geomicrobiology, NRFeOx, aquifer, groundwater, iron metabolism, iron oxidizers, nitrate, pyrite

High concentrations of nitrate (NO_3^-) in groundwater cause negative effects on both human health and the environment (1, 2). In agricultural areas, nitrate is mostly derived from application of nitrogen-based chemicals and organic fertilizers (3). This nitrate input can lead to excessive nitrate concentrations that are responsible for low groundwater quality and pollution of drinking water supplies (4, 5). The guideline value for nitrate present in freshwaters set by the World Health Organization and the European Union to protect groundwater is 50 mg/liter (Drinking Water Directive 98/83/EC [2]). Therefore, water remediation and nitrate removal are necessary to protect public health and the entire ecosystem.

Industrial technologies for nitrate removal from drinking water include approaches divided into separation-based and elimination-based methods. Many of those methods are considered inefficient and expensive or may generate hazardous concentrated waste that requires careful disposal (6, 7). In natural ecosystems, nitrate removal is usually mediated in the absence of oxygen or at low oxygen concentrations by different microbial processes. In denitrification, nitrate is reduced stepwise to dinitrogen (N_2) gas. Denitrifying bacteria mediate a series of sequential reduction reactions as follows: $NO_3^- \rightarrow NO_2^- \rightarrow NO \rightarrow N_2O \rightarrow N_2$. Gaseous intermediates and end products are released to the atmosphere. A second process, called dissimilatory nitrate reduction to ammonium (DNRA), results in the production of ammonium and the retention of nitrogen in the ecosystem (8). The factors that may determine the activity of these different pathways are, e.g., pH, sulfide concentrations, the type and complexity of the electron donors, the bioavailability of electron acceptors, and the resulting ratio of carbon to nitrate (9). Under carbon-limited conditions, when the ratio is low, denitrification is favored over DNRA (10, 11). Most of the microbial denitrifiers described so far are heterotrophs and therefore need an organic carbon source to be able to reduce nitrate (12). However, in oligotrophic systems, such as many aquifers, bacteria are often limited in organic carbon compounds, which influences the potential of microbially mediated nitrate reduction and inhibits the activity of heterotrophs (13, 14).

In addition to organic matter, denitrifying microorganisms can also utilize various inorganic electron donors, such as iron(II), reduced sulfur compounds, H_2, or even U(IV) (15). Bacteria that require organic carbon in addition to iron(II) as a cosubstrate (e.g., acetate) are called mixotrophic nitrate-reducing iron(II)-oxidizing (NRFeOx) bacteria (16–19). It seems that none of the well-studied mixotrophic strains are actually able to oxidize Fe(II) enzymatically (20). Instead, most of them probably cause Fe(II) oxidation by triggering an abiotic reaction of Fe(II) with reactive nitrogen species that are byproducts of heterotrophic denitrification (21, 22). Therefore, they are not considered true mixotrophs and instead have been called chemodenitrifiers (20, 23). Purely autotrophic NRFeOx bacteria such as the lithoautotrophic NRFeOx culture KS (named after Kristina Straub), enriched about 2 decades ago from a freshwater sediment (24–26), were shown to use only inorganic carbon (HCO_3^-) to build biomass and enzymatically mediate the oxidation of iron(II) coupled to the complete reduction of NO_3^- (15, 20, 27) according to the following reaction.

$$10Fe^{2+} + 2NO_3^- + 24H_2O \rightarrow 10Fe(OH)_3 + N_2 + 18H^+ \quad (1)$$

This process requires reducing conditions where iron(II) is present as dissolved Fe^{2+}(aq) or as a component of iron(II)-bearing minerals (28), such as iron sulfides, e.g., pyrite (FeS_2) (29, 30). Pyrite is often a prevalent accessory constituent of carbonate-rock (limestone, dolomite) aquifers and can serve as a source of reduced sulfur species and iron(II), promoting iron-dependent chemolithoautotrophic denitrification (13, 31,

32). A number of studies link pyrite oxidation to nitrate reduction (33–38) and emphasize the importance of the NRFeOx process in freshwater aquifers (39–45). Despite the environmental relevance, to date no lithoautotrophic NRFeOx bacteria have been isolated or even enriched from an oligotrophic aquifer, and as such, there are no model cultures to study the biogeochemistry of this potentially environmentally relevant process.

The objectives of the present work therefore were (i) to enrich a lithoautotrophic Fe(II)-oxidizing denitrifying culture from a pyrite-rich and nitrate-contaminated aquifer and (ii) to determine the rates of nitrate reduction coupled to iron(II) oxidation. We further intended (iii) to evaluate the capacity of the culture to perform continued autotrophic denitrification coupled to iron(II) oxidation over several growth transfers and (iv) to characterize the microbial community in the enrichment culture.

RESULTS AND DISCUSSION

Identity of the enriched lithoautotrophic NRFeOx culture. Primary enrichment cultures from microbial trapping devices (MTDs) were incubated at room temperature in the dark and transferred to fresh medium every 2nd to 3rd week, when the cultures turned visually orange and dissolved Fe^{2+} was completely oxidized. In 7 out of 10 cultures, we observed Fe(II) oxidation and cell growth; 1 of these 7 was selected for further transfers and characterization. After 21 continuous transfers under neutrophilic Fe(II)-oxidizing and nitrate-reducing conditions with 2 mM Fe(II) as the only electron donor, 2 mM nitrate as the only electron acceptor added, and CO_2 as the only carbon source, it was evident that the enriched microbial culture does not require any addition of organic carbon to sustain cell growth and therefore can be considered a potentially lithoautotrophic culture. To our best knowledge, the enriched culture is only the third known lithoautotrophic NRFeOx culture that was shown to be continuously transferred under lithoautotrophic conditions, besides culture KS (24) and the recently described culture BP (named after the location of isolation, Bremen Pond) (46). In addition, it is the only known lithoautotrophic NRFeOx culture enriched from an oligotrophic aquifer. Long-read 16S rRNA gene amplicon sequencing of the microbial community in the culture showed that it is dominated by *Betaproteobacteria*, with the highest relative abundance of bacteria belonging to the *Nitrosomonadales* order, related to the *Gallionellaceae* family (49%) (Fig. 1A.). Members of this family are known as obligate microaerophilic bacteria capable of autotrophic growth with Fe(II) as electron and energy source (47).

Analysis of the long-read 16S rRNA gene analysis furthermore revealed that the dominant *Gallionellaceae* sp. in our culture has only 96.24% and 96.17% sequence similarity to the next closely related, cultured microorganisms, *Ferrigenium kumadai* and *Gallionella capsiferriformans* ES-2, respectively. This suggests that the enriched microorganisms might represent a new species or genus within the *Gallionellaceae* family. Due to the limitation of 16S rRNA in gene comparison for novel taxa, the whole genome needs to be obtained for further phylogenic analysis. Closely related sequences were previously found in *in situ* communities in aquifers and mineral springs of groundwater (Fig. 1B). Additionally, bacteria belonging to the *Gallionellaceae* family were found to dominate the microbial community present in the groundwater monitoring well from which our culture was enriched, with up to 50% relative abundance of the population (Blackwell et al., unpublished data). This implies that *Gallionellaceae* spp. may be important members in freshwater communities and that their environmental role should be investigated further using meta-omics studies.

The other culture for which lithoautotrophic Fe(II) oxidation coupled to nitrate reduction has been demonstrated unequivocally is culture KS, enriched from a freshwater ditch in Bremen, Germany (24). Similar to our NRFeOx culture, culture KS is dominated by bacteria affiliated with the *Gallionellaceae* family (25, 48); however, the most abundant presumed Fe(II) oxidizer (*Gallionellaceae* sp.) from culture KS is 97.06% similar based on 16S rRNA gene sequence analysis to the *Gallionellaceae* sp. from this study. Recent metagenomic studies of culture KS further revealed that in this culture, *Gallionellaceae* sp. is

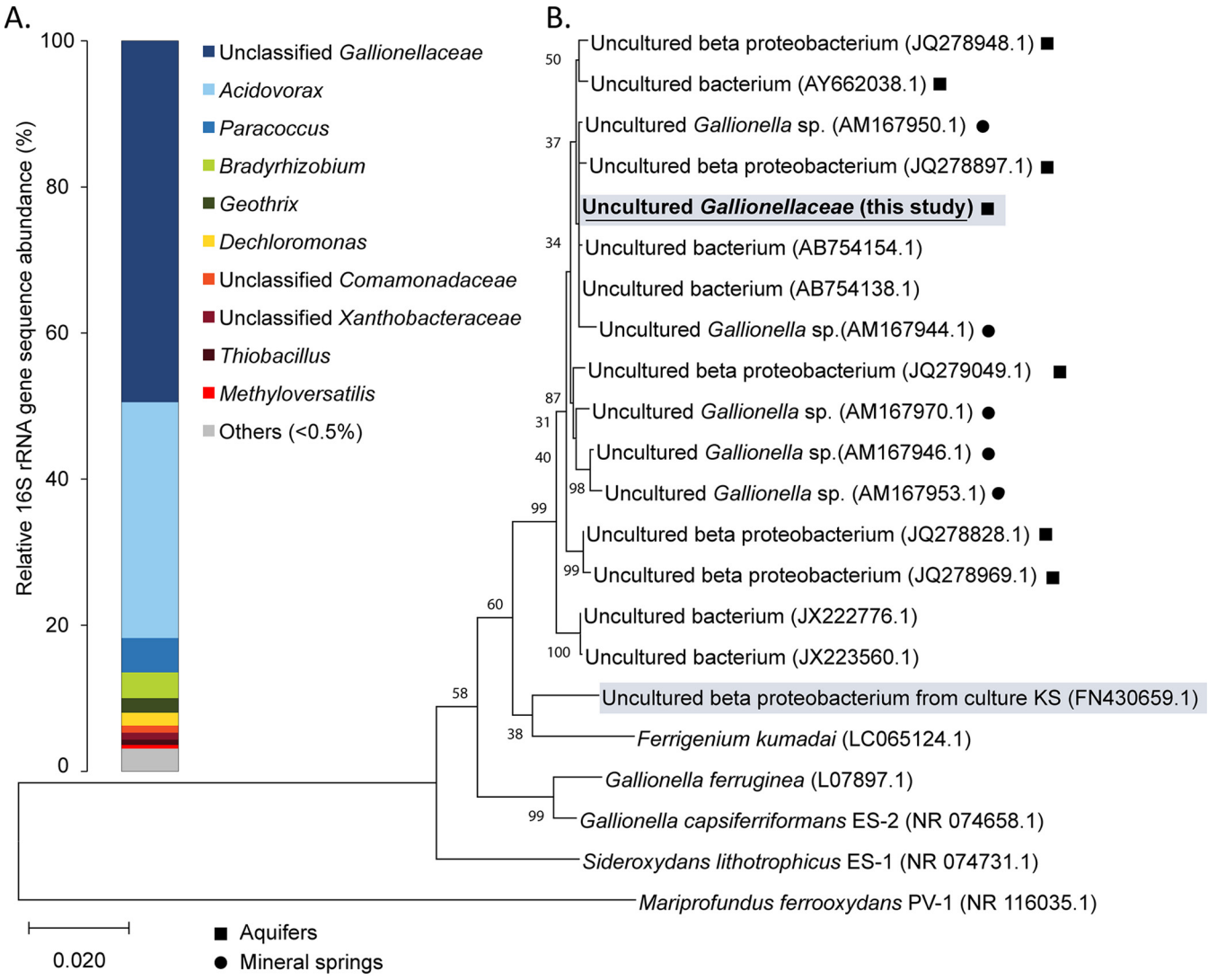

FIG 1 Relative abundance of taxa (A) found in the autotrophic NRFeOx enrichment culture based on long-read 16S rRNA gene sequences, where sequence similarities to cultured representatives at family and genus level ranged from 96% to 100% (query coverage >99%), based on SINAsearch (86) using the SILVA 132 database. Neighbor-joining phylogenetic tree (B) constructed showing the relation of the most dominant bacterium in the enrichment culture (blue background, bold and underlined) and representative microaerophilic Fe(II) oxidizers related to *Gallionella* spp. and *Sideroxydans* sp. including the most abundant representative of *Gallionellaceae* family present in culture KS (blue background). *Mariprofundus ferrooxydans* PV-1, a microaerophilic Fe(II) oxidizer, was included as outgroup. The scale bar corresponds to 0.02 nucleotide substitutions per site. At the branches, high-confidence (>50) bootstrap values (from 1,000 replications) are shown. GenBank accession numbers are shown in parentheses next to the organism names. Squares indicate bacteria enriched from aquifers, and circles indicate bacteria originating from mineral springs.

lacking NO and N_2O reductase genes, suggesting that, as complete denitrification is occurring in the culture (based on stoichiometry), toxic NO must be consumed and then converted to N_2 by other flanking community members (potentially heterotrophic NO and N_2O reducers). *Gallionellaceae* sp. in the culture KS probably utilizes cyc2, MtoAB system, or OmpB to transfer electrons from Fe(II) to cytochromes present in the inner membrane to reduce the quinone pool. Reduced ubiquinol could then be passed to the nitrate reductase in one direction for energy generation and in the other direction to generate NAD(P)H for carbon fixation. Therefore, as an autotroph, *Gallionellaceae* sp. may later support the community by providing reducing equivalents (potentially as organic carbon) for complete denitrification (49). This suggests that an efficient cooperation between *Gallionellaceae* sp. and other strains present in the culture KS guarantees robust and continuous chemolithoautotrophic NRFeOx. Similar observations were made recently for another autotrophic enrichment NRFeOx culture, also originating from freshwater sediments (culture BP), which like the KS culture and the culture presented here is also dominated by a member of the

Gallionellaceae family. The metagenome-assembled genome of *Gallionellaceae* sp. from BP culture lacks NO_3^- and N_2O reductases, and therefore complete nitrate reduction and Fe (II) oxidation occurring in this culture were suggested to result from a complex network of microbial interactions among several Fe(II) oxidizers and denitrifiers rather than by the activity of one species (46). However, it should be noted that since the amplicon sequence variants (ASVs) of *Gallionellaceae* spp. in KS, BP, and the culture presented here are different, the genomic traits and the roles they play in the community may differ.

The second most abundant bacterium present in our culture also belongs to the *Betaproteobacteria* and was affiliated with *Acidovorax*. Some species of this genus, such as *Acidovorax ebreus*, *Acidovorax* sp. strain 2AN, or *Acidovorax* sp. strain BoFeN1, were found to be proficient at mediating nitrate-dependent iron(II) oxidation (17, 50, 51). However, at least *Acidovorax* strain BoFeN1 was shown not to be a true mixotrophic nitrate-dependent iron(II) oxidizer [using both Fe(II) and the organic cosubstrate as electron sources] but instead to produce nitrite during heterotrophic denitrification, causing an abiotic oxidation of the Fe(II) (chemodenitrification) (17, 21). Nevertheless, the *Acidovorax* sp. in our enrichment might potentially also play an important role in nitrate turnover [and maybe to a small extent in Fe(II) oxidation] by oxidizing organic carbon provided by the autotrophs.

In addition to iron(II) oxidizers, other community members in our enrichment culture have 16S rRNA gene sequences most similar to those of bacteria known as nitrate reducers, such as *Rhodocyclaceae* (2.75%), which is closely related to *Dechloromonas* spp. that are often dominant in denitrifying populations in sediments (52–54), including strain UWNR4 obtained from river sediments that oxidizes Fe(II) in the presence of nitrate and acetate (55). Some ASVs were assigned to be closely related to other nitrate-reducing taxa such as *Bradyrhizobium* spp. (56, 57) belonging to *Xanthobacteraceae* (5.8%). Interestingly, *Bradyrhizobium* is also present in culture KS and was found to possess RuBisCO genes that can be used to fix CO_2. If so, *Bradyrhizobium* in culture KS is likely conducting Fe(II) oxidation coupled with denitrification to obtain reducing equivalents and ATP needed for CO_2 fixation (48). Our culture comprises microorganisms related to a *Geothrix* sp. (2%) (*Holophagaceae*), a potential iron(III) reducer also found previously in aquatic environments such as aquifers (58). The presence of iron(III) reducers suggests the possibility for iron cycling in the culture using internally produced organic compounds.

Physiology of the enriched lithoautotrophic NRFeOx culture. To measure rates of denitrification coupled to iron(II) oxidation, the lithoautotrophic NRFeOx enrichment culture was cultivated continuously on fresh medium containing Fe(II) and NO_3^- as the only electron donor and acceptor. The cultivation was repeated over three transfers, i.e., the first transfer (generation of the culture) was used to inoculate the second that was then used to inoculate the third. Since no organic carbon sources were provided externally to the denitrifying culture, and since we observed Fe(II) oxidation, nitrate reduction, and growth of cells over time, the reduction of nitrate must be mediated by microorganisms and is mainly linked to iron(II) oxidation. An addition of 2 mM $FeCl_2$ and 2 mM nitrate (molar ratio of 1:1, representing the electron acceptor, i.e., nitrate, in excess) to sodium carbonate buffered low phosphate medium was followed by iron(II) carbonate and iron(II) phosphate precipitation, which resulted in a final concentration of ca. 1.3 mM Fe^{2+}(aq). Oxidation of total Fe(II) was never complete, but it ceased when approximately 90% of the added iron was oxidized (Fig. S3 and S4). In contrast, dissolved Fe^{2+}(aq) was always completely removed (i.e., oxidized) after each transfer (Fig. 2). The reason for that could be the difference in bioavailability of Fe(II) in aqueous and solid form, i.e., precipitation of siderite and vivianite might lead to formation of Fe (II) solids which the culture is unable to use as electron donor. Per 1 mM oxidized Fe(II), the NRFeOx culture formed 6.9×10^5 cells/ml (Fig. S5).

Because Fe(II) oxidation by truly autotrophic NRFeOx bacteria is enzymatic, mediated by a dedicated Fe(II) oxidase, and probably happening in the cell periplasm (48, 50), we specifically only present the removal of Fe^{2+}(aq) here, i.e., the Fe species that can enter the periplasm. Additional plots showing concentrations of total Fe(II) over

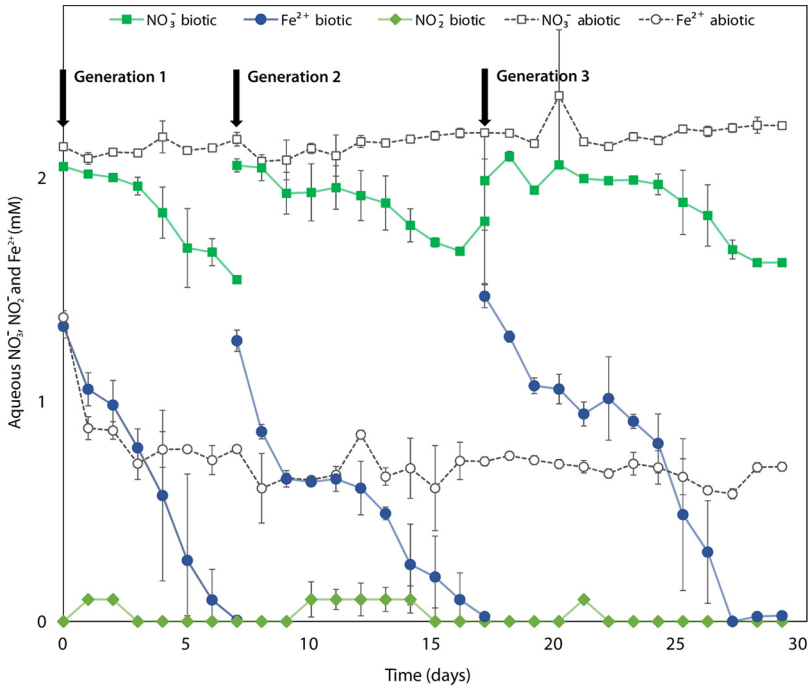

FIG 2 Concentrations of dissolved NO_3^-, NO_2^-, and Fe^{2+} in three consecutive transfers of the enriched autotrophic nitrate-reducing, Fe(II)-oxidizing culture. All data points are mean values of samples from three replicate bottles; error bars represent standard deviations. The transfers on days 0, 7, and 17 are indicated by arrows.

time are presented in the supplemental material (Fig. S3). The overall rates of NO_3^- reduction and removal of Fe^{2+}(aq) [most probably by oxidation as indicated by the stoichiometric formation of Fe(III); Fig. S3] were similar over all three consecutive transfers, showing the reproducibility of the microbially catalyzed process. Complete removal of Fe^{2+}(aq) occurred within 7 to 11 days at the expense of nitrate, i.e., the culture reduced 0.3 to 0.5 mM nitrate and oxidized 1.3 to 2 mM Fe^{2+}(aq). Generally, Fe^{2+}(aq) conversion can be divided into three phases (Fig. 2). In phase 1 (0 to 2 days after inoculation), the decrease of Fe^{2+}(aq) concentration (0.40 ± 0.08 mM) was always observed immediately after addition of Fe(II) to the medium followed by inoculation, which may be associated with the precipitation of siderite and vivianite and the sorption of the iron(II) to the glass wall. This might be supported by the fact that the same decrease of iron(II) concentration (ca. 0.5 mM) was also observed in abiotic controls between days 0 and 1 (first transfer) (Fig. 2). The same noninoculated bottles were used as an abiotic control for the two subsequent transfers; therefore, no further fluctuation in substrate concentrations in the abiotic controls was found. After approximately 2 days (2nd phase), Fe^{2+}(aq) oxidation slowed down, which may be related to a microbial adaptation phase or potentially also to NO_2^- production and the resulting lowering or even inhibition of the Fe(II) oxidase activity due to nitrite toxicity (34, 59, 60). However, although we observed the accumulation of nitrite, it was minor and never exceeded 0.1 mM. In contrast, nitrite accumulation in nitrate-dependent iron(II)-oxidizing cultures at millimolar concentrations has been described previously by Kappler et al. (17) for *Acidovorax* strain BoFeN1 and by Weber et al. (61) for *Pseudogulbenkiania* sp. strain 2002. These two strains cannot grow purely autotrophically with Fe(II) and nitrate but are known to require an additional organic substrate or at least precultivation on organic substrate (62) that probably leads to internal carbon storage and heterotrophic denitrification, nitrite formation, and chemodenitrification. However, nitrite in pure cultures of strain BoFeN1 and strain 2002 remained in solution until the end of incubation, whereas in our culture, nitrite was always low and had

TABLE 1 Decreases of NO_3^- and Fe(II) concentrations, rates, and stoichiometries of NO_3^- reduction and Fe(II) oxidation in three transfers of the microcosm experiment

Transfer number	Culture number	Rate of NO_3^- reduction (mM/day)	Rate of Fe(II) oxidation (mM/day)	Rate of Fe^{2+}(aq) oxidation (mM/day)	Ratio of $NO_3^-{}_{reduced}$/ $Fe(II)_{oxidized}$	Ratio of $NO_3^-{}_{reduced}$/ $Fe^{2+}(aq)_{oxidized}$
1	1.1	0.12	0.39	0.27	0.31	0.45
	1.2	0.08	0.30	0.25	0.22	0.30
	1.3	0.05	0.30	0.18	0.23	0.26
	Avg	0.08 ± 0.03	0.33 ± 0.04	0.24 ± 0.04	0.26 ± 0.04	0.33 ± 0.08
2	2.1	0.04	0.14	0.14	0.32	0.32
	2.2	0.05	0.18	0.13	0.22	0.34
	2.3	0.04	0.19	0.19	0.21	0.21
	Avg	0.04 ± 0.00	0.30 ± 0.02	0.15 ± 0.03	0.25 ± 0.05	0.29 ± 0.06
3	3.1	0.05	0.17	0.22	0.28	0.21
	3.2	0.05	0.18	0.22	0.26	0.22
	3.3	0.05	0.20	0.23	0.25	0.23
	Avg	0.05 ± 0.00	0.25 ± 0.01	0.22 ± 0.00	0.26 ± 0.01	0.22 ± 0.01

been completely removed by the end of the incubation. The complete removal of nitrite in our culture may be explained by the presence of denitrifying bacteria potentially equipped with nitrite reductases which might have used internally produced carbon compounds derived by primary biomass producers. However, a part of the nitrite could also have been reduced by an abiotic reaction with iron(II) (63, 64). Additionally, the presence of Fe(II) minerals like siderite (65) could have catalyzed the process by providing reactive surfaces (66). The 3rd phase of the incubation (last 5 to 6 days) was characterized again by rapid removal, i.e., oxidation, of Fe^{2+}(aq) in the biotic setups with a maximum Fe^{2+} removal rate of 0.5 ± 0.1 mM/day. The multistage nature of the process might be related to the accessibility to Fe^{2+}(aq), which is limited by dissolution of solid phases present in the medium (siderite, vivianite), or to inhibitory effects of the accumulated nitrite. In the abiotic controls, no changes in nitrate, nitrite, or Fe(II) concentrations were observed within the time of the experiment.

The average $nitrate_{reduced}$/total $Fe(II)_{oxidized}$ ratio over three transfers of 0.28 ± 0.1 (Table 1) is slightly higher than but still approximates the theoretical stoichiometry of Equation 1, suggesting almost complete reduction of NO_3^- to N_2. Similar ratios were shown for culture KS growing autotrophically (26), yielding ratios of 0.21 to 0.24, and in a marine sediment microcosm study (67) in which a $nitrate_{reduced}/Fe(II)_{oxidized}$ ratio of 0.22 to 0.28 was measured. This suggests that less Fe(II) is oxidized or slightly more nitrate is removed than expected from the 1:5 ratio of nitrate (reduced) and Fe(II) oxidized. In fact, the theoretical ratio should be even lower than 0.2 because some of the electrons from Fe(II) oxidation must also be used for the reduction of CO_2 (for biomass production) rather than reduction of nitrate (for energy generation) (67). In our setups amended with ^{15}N-$NaNO_3^-$, from the 0.61 mM ^{15}N-nitrate that was removed, 0.11 ± 0.02 mM nitrate was reduced to ^{15}N-N_2, while 0.25 ± 0.01 mM was reduced to ^{15}N-N_2O (Table S1). If directly coupled to autotrophic Fe(II) oxidation, these reactions would lead to oxidation of ca. 1.55 mM Fe(II) of the initial 2.0 mM Fe(II). This suggests that with the remaining 0.45 mM Fe(II) (that was also oxidized based on our geochemical analyses), ca. 0.25 mM nitrate could have been converted to ^{15}N-NO (or maybe also ^{15}N-NH_4^+), which both were not measured in the ^{15}N isotope analyses. Quantification of dissolved ammonium by flow injection analysis (FIA) showed that its overall concentration decreased over time of incubation from 5.52 ± 0.01 to 5.38 ± 0.06 mM (Fig. S7), meaning that if any ammonium was produced due to nitrate reduction, its concentration was lower than the amount of ammonium that was consumed by the microbes during the incubation. Overall, this shows that nitrate removal by the studied NRFeOx culture results from multiple metabolic reactions in which both Fe(II) and, to a small extent, organic carbon

compounds are used as electron donors. Potential sources of organic carbon for nitrate reduction by the heterotrophic bacteria are internally produced organic carbon by the autotrophic Fe(II) oxidizers (leading to cross-feeding) or traces of organic carbon present as a background contaminant in Milli-Q water used for medium preparation (measured to be in the range of 0.3 to 0.9 mg/liter). Additional explanations for the extra nitrate consumption are the storage of nitrate in the cells or maybe also the use of nitrate as an N source for assimilation. In order to verify to which extent the culture can grow solely on nitrate and organic carbon stemming from the background in the water, the culture was inoculated in the same medium with nitrate but without any addition of Fe(II). As controls, separate microcosms with nitrate and 1, 2, and 3 mM Fe(II) were used. Bacteria in setups with no Fe(II) reduced 0.24 ± 0.06 mM nitrate, i.e., less than in incubations with 1 mM Fe(II) (0.36 ± 0.03 mM) (Table S2; Fig. S5C and D). In setups where 2 mM and 3 mM Fe(II) was added, the amount of nitrate reduced was higher and reached 0.61 ± 0.04 and 0.76 ± 0.03 mM, respectively. Interestingly, in all microcosms where Fe(II) was present, the ratio of $\text{nitrate}_{\text{reduced}}/\text{Fe(II)}_{\text{oxidized}}$ was again between 0.24 and 0.33, independent of Fe (II) concentration (Table S2). In addition, cell numbers were counted at the beginning (day 0) of the experiment and at day 5, respectively, when reduction of nitrate and/or oxidation of Fe(II) has stopped. The results (Table S3) show that the final number of cells growing in the cultures with Fe(II) was higher than that of cells growing in setups with no Fe(II), although there was no statistically significant pair of treatments (P value = 0.76). These results show that direct coupling of nitrate reduction to Fe(II) oxidation ultimately results in carbon fixation, leading to biomass production, which is favorable for the community as a whole but is not necessarily mediated by all members of the community. To confirm this result and to clearly demonstrate autotrophic growth, we performed an additional experiment with several sequential spikes of Fe(II) that are expected to lead to additional cell growth after each spike. For this experiment, incubations were prepared using the same medium amended with 2 mM Fe(II), 2 mM NO_3^-, and 10% (vol/vol) of inoculum as described above but with a difference that once all Fe(II) had been completely oxidized, the same bottles were spiked with additional 2 mM Fe(II). Three continuous Fe(II) oxidation phases were carried out to follow cell numbers. Since all trace carbon stemming from the water should be consumed in the initial incubation, all nitrate reduction in the 2nd and 3rd phase [after the 2nd and 3rd spike with Fe(II)] can be attributed to Fe(II) oxidation only. As expected for a culture performing autotrophic Fe(II) oxidation coupled to nitrate reduction, the spiking experiment indeed resulted not only in an enhanced rate of Fe(II) oxidation after the 2nd and 3rd spike of Fe(II) but in particular in an incremental increase in cell numbers after each spike of Fe(II), resulting in $7.73 \times 10^6 \pm 4.37 \times 10^5$ cells/ml at the end of incubation (Fig. S6.).

Cell-mineral interactions. As a consequence of Fe(II) oxidation, Fe(III) mineral precipitates were formed. Mössbauer spectroscopy identified the formation of a short-range ordered Fe(III) (oxyhydr)oxide mineral phase with hyperfine parameters that were similar to those of ferrihydrite (Table S4; Fig. 3B) (68). Mössbauer data also revealed that up to 10% of Fe(II) remained in the precipitate. X-ray diffraction was unable to resolve any clear reflections corresponding to any Fe mineral (Fig. 3A) which, combined with the results of the Mössbauer data, provides clear evidence that ferrihydrite was the formation product of microbial Fe(II) oxidation. Scanning electron micrographs and light microscopy images of the NRFeOx culture showed that bacteria are closely associated with the Fe(III) precipitates but that only a few of the cells were encrusted in minerals at the end of the Fe(II) oxidation phase (Fig. 4). This suggested that most of the cells are able to avoid mineral precipitation at their cell surface. Several possible mechanisms have been suggested in the literature to explain how cells can avoid encrustation, e.g., via excretion of Fe(III)-complexing ligands that can retain Fe(III) in solution or by maintaining a slightly acidic microenvironment around cells (19, 69–71). For the cells present in our culture, the change of pH could be local (in the direct cell environment) since the overall pH of medium did change only to a minor extent during the incubation time (decrease from 7.04 ± 0.00 to 6.93 ± 0.03).

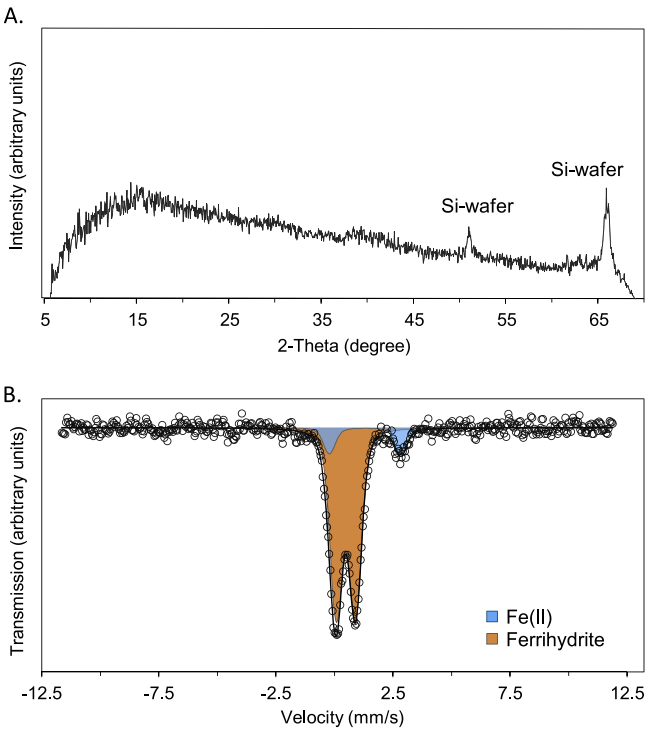

FIG 3 X-ray diffractogram (A) and Mössbauer spectrum (B) of the minerals formed during oxidation of 2 mM Fe(II) by the Fe(II)-oxidizing, nitrate-reducing enrichment culture. Samples were taken after 11 days. The diffraction reflexes at 51.0°2θ and 65.9°2θ belong to Si-wafer (sample holder). In the Mössbauer spectrum, the black circles indicate raw data, the brown area represents short-range ordered Fe(III) oxyhydroxide, likely ferrihydrite, and the blue-shaded represents Fe(II).

The culture, however, was observed to perform nitrate reduction coupled to Fe(II) oxidation also at lower pH values of 6.0 and 6.5 (Fig. S5A and B), showing that the cells were capable of metabolizing under these lower-pH conditions. Additionally, such an acidification of the local environment around cells may also stimulate the dissolution of carbonates such as siderite (71). This may have important implications for the environments where siderite or iron-bearing carbonates are present (e.g., in carbonate-rich aquifers) and may serve as an Fe(II) source for chemolithotrophic bacteria.

Relevance of *Gallionellaceae*-related strains for Fe(II) oxidation in anoxic, nitrate-rich environments such as aquifers. Knowledge of the microbial key players, the mechanisms, and the controlling factors of anaerobic nitrate-reducing Fe(II) oxidation is critical for understanding the fate of nitrate, one of the pollutants in groundwater aquifers. Under *in situ* conditions, rates of NRFeOx can be controlled by various process-limiting factors. Depending on the aquifer, either the electron acceptor nitrate (determined by the input from agriculture) or the electron donor [Fe(II), potentially limited by the solubility of the available Fe(II)-containing minerals] can limit the NRFeOx process, while the carbon source, CO_2, is usually not limiting in such systems. This is supported by numerous environmental studies, which provided evidence for the importance of autotrophic processes mediated by microorganisms in the subsurface. As an example, in one previous study where the response of an aquifer microbial community to an increase in the flux of electron acceptor, i.e., nitrate, was characterized, metatranscriptomic data showed an unexpected increase of the activity of *Gallionellaceae* spp. [known autotrophic microaerophilic Fe(II) oxidizers], although the influx of a thermodynamically favorable electron acceptor like nitrate was expected to stimulate microbial oxidation of organic electron donors (41). In the studied aquifer, Fe(II) originates mainly from mineral phases such as pyrite, Fe(II)-bearing carbonates, and clays. The maximum concentration of aqueous Fe^{2+} measured in groundwater was 0.02 mM. The availability of aqueous Fe^{2+} is therefore determined by the solubility of Fe(II) minerals

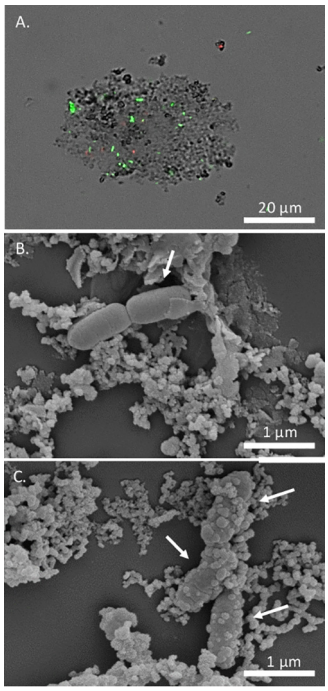

FIG 4 Overlay of fluorescence and transmission light microscopic pictures of the autotrophic NRFeOx culture enriched in this study. Cells were stained with the LIVE/DEAD stain (green, alive; red, dead) (A). Scanning electron micrographs of the culture after 11 days of incubation showing nonencrusted (B) and encrusted (C) cells. Arrows indicate cells.

and activity of sulfide-oxidizing microorganisms, like potentially *Thiobacillus* sp. present in this culture. However, some microorganisms can directly oxidize Fe(II)-containing minerals. For instance, an *mto* gene cluster that forms a pathway that couples extracellular oxidation of Fe(II) to the reduction of quinone to quinol in the cytoplasmic membrane has been found in *Sideroxydans lithotrophicus* ES-1 (*Gallionellaceae family*) (72). This indicates that some representatives of this family have the metabolic potential to directly oxidize solid iron(II) phases. The same bacterial strain, *Sideroxydans lithotrophicus* ES-1, was also observed in high abundance in the rock-attached communities of passive samplers incubated in a pristine limestone aquifer, along with other potential autotrophs related to *Thiobacillus* (13). Taken together with our results, these findings highlight the potential importance of chemolithoautotrophic bacteria in linking biogeochemical cycles of N, C, S, and Fe species in aquifers and raise the question about the exact role of typically microaerophilic iron(II)-oxidizing *Gallionellaceae*-related bacteria in mediating denitrification under anoxic conditions. The isolation of an individual strain of the relevant *Gallionellaceae* sp. from the nitrate-dependent iron(II)-oxidizing cocultures KS, BP, and the enrichment culture presented here, together with genome analyses, is the key for future studies to understand the ecological importance of NRFeOx in natural environments, in particular groundwater aquifers.

MATERIALS AND METHODS

Field site and sampling. The studied aquifer is located in southwest Germany (Baden-Württemberg) and is the major drinking water supply across the Ammer catchment. The land use of this catchment at the regional scale is homogeneous, with about 67% of the area being used for agriculture. The geological setting of the aquifer is dominated by Triassic carbonates of the Upper Muschelkalk. Fractured bedrock consists of dolomitic, micritic, and bioclastic pyrite-bearing limestones (73) with a pyrite concentration of 4.1 $\pm$ 1.4 mg/g of rock (determined by the AVS/CRS method, see supplemental material). Groundwater is accessible for sampling via production wells and monitoring wells, which have a broad range of nitrate concentrations (Fig. S1). The median nitrate concentrations in the monitoring wells located in uncovered Muschelkalk layers are between 29.8 and 38.3 mg/liter (0.35 and 0.45 mM). Similar or slightly higher concentrations of 42.5 to 54.4 mg/liter (0.5 to 0.64 mM) were observed at the karstic spring of the Ammer river that integrates over part of the catchment. Based on that, we hypothesized that the changes of nitrate

concentration were driven mainly by *in situ* transformations and that low-nitrate concentrations were indicators of potential hot spots of microbial nitrate turnover. A low-nitrate anoxic artesian well (48° 33′47.52′′N, 8°53′59.279′′E) was therefore selected for the enrichment of microbial key players involved in nitrate removal. During the observation period (2004 to 2018), the average nitrate concentration ($n = 8$) was 1.5 ± 0.6 mg/liter (0.02 ± 0.01 mM), with a mean conductivity of 885.1 ± 75.1 μS/cm ($n = 9$), a circumneutral pH of 7.1 ± 0.1 ($n = 9$), and an average temperature of 12.5 ± 1.6°C ($n = 9$). The groundwater well had anoxic to suboxic conditions (dissolved O_2 of 0.1 ± 0.1 mg/liter, $n = 4$) and a mean dissolved organic carbon (DOC) concentration of 1.2 ± 0.3 mg/liter ($n = 4$).

Microbial communities used for enrichment cultures were sampled using passive samplers called microbial trapping devices (MTDs) (adapted from previous publications [13, 74, 75]) filled with representative *in situ* rock material (Fig. S2). Fresh pyrite-bearing limestone was collected from Upper Muschelkalk outcrops, crushed with a hammer and a jaw crusher to 3-mm fragments, sterilized by autoclaving under anoxic conditions to minimize mineral transformations, and exposed to UV light (8 W, S/L; Herolab GmbH Laborgeräte, Germany, UVC at 254 nm, exposure time 1 h). Rock particles were then transferred into sterile 10-cm-long Teflon tubing with 2-mm-diameter randomly distributed holes (Fig. S2). Rock material was fixed with sterile glass wool on both sides of the tubing to prevent loss of the material. MTDs were attached to a stainless-steel wire, deployed into the artesian well to the depth were water-conducting fractures were found (29 to 35 m below the ground) by deploying a camera into the well, and incubated for 4 months. This approach enabled the enrichment of microorganisms inhabiting pyrite-rich limestone that is building the aquifer. After incubation, the MTDs were collected, transferred to sterile anoxic jars filled with N_2, and stored wet for 4 weeks at 4°C in the dark until enrichment cultures were set up.

Setup of microbial enrichments and incubation conditions. Rock material with attached microbial communities obtained from incubated MTDs was distributed in a glove box (100% N_2), and approximately 4 g were then transferred into separate sterile serum bottles (58 ml) that were filled with 25 ml of anoxic bicarbonate-buffered (22 mM) low phosphate medium (LPM), adjusted to pH 7.0 to 7.1 (69). The concentration of selenite-tungstate solution (76) was decreased from 1.0 ml/liter to a final concentration of 0.1 ml/liter to eliminate a potential inhibitory effect of tungsten on the nitrate reductase, as it was reported previously by Burke et al. (77). Bottles were closed with butyl-rubber stoppers and crimped, and the headspace was flushed with N_2/CO_2 (90:10). After this step, bottles were amended with 2 mM $NaNO_3$ and 2 mM $FeCl_2$. Adding Fe(II) was followed by the precipitation of vivianite and siderite (78) that resulted in a final concentration of ca. 1.3 mM dissolved iron(II), i.e., Fe^{2+}(aq). Enrichments were incubated at room temperature in the dark and transferred to fresh medium every 2 to 3 weeks (for about a year in total) after complete oxidation of iron(II).

For quantification of rates and the extent of nitrate-dependent iron(II) oxidation, medium was prepared as described above (2 mM $NaNO_3$, 2 mM $FeCl_2$ [pH 7.0 to 7.1]) and inoculated with 10% (vol/vol) of the NRFeOx enrichment culture (that was cultivated over 21 subsequent transfers under lithoautotrophic conditions). Once at least 90% of Fe(II) had been oxidized, the microbial culture was transferred to fresh medium. Three continuous transfers were carried out to follow rates of Fe(II) oxidation and nitrate reduction over these three successive transfers. Sterile setups were used as controls. All cultures and abiotic controls were conducted in triplicates and incubated at room temperature in the dark. Final rates and ratios were calculated as an average of rates and ratios from each individual replicate.

Additionally, to analyze the gaseous products of nitrate reduction coupled to Fe(II) during growth of the autotrophic NRFeOx enrichment culture, a separate experimental setup was run using the same medium, substrates, and inoculum volume as described above, except the medium was amended with ^{15}N-labeled $NaNO_3^-$ (for details see supplemental material).

Cell counts, light microscopy, and scanning electron microscopy. Cell numbers were quantified using an Attune NxT flow cytometer (Thermo Fisher Scientific) equipped with a blue laser beam as an excitation source (488 nm). Prior to flow cytometry, an aliquot of the cells was stained using BacLight green stain (Thermo Fisher Scientific). Cells were distinguished from debris by their properties in the side-scatter and fluorescence parameters. All measurements were conducted in triplicates and the results were reported as an average. A two-way analysis of variance (ANOVA) test was used to test the effects of Fe(II) concentration on cell numbers using R (79).

Transmission light and fluorescence microscopy was performed with a Leica DM5500 B epifluorescence microscope equipped with a 40× air objective (numerical aperture, 0.75). The filter sets applied were L5 (excitation filter, band-pass [BP] 480/40 nm; dichromatic mirror, 505 nm; suppressor filter, BP 527/39) and Y3 (excitation filter, BP 543/30; dichromatic mirror, 565 nm; suppressor filter, BP 610/75). Cells were stained with the LIVE/DEAD BacLight bacterial viability kit (Molecular Probes, Carlsbad, CA, USA). For scanning electron microscopy (SEM), samples were fixed with glutaraldehyde (2.5% final concentration) and left at 4°C overnight. A stepwise dehydration was performed by an ethanol dilution series with increasing ethanol concentrations (30%, 75%, 95%, and twice 100%). Samples were then treated with hexamethyldisilazane (HMDS; Sigma-Aldrich, St. Louis, MO, USA) (80). Micrographs were collected at the Centre for Light-Matter Interaction, Sensors & Analytics ($LISA^+$), University of Tübingen. JEOL JSM-6500F field emission SEM with a Schottky-field-emitter were used. Working distances were approximately 10 mm, and the acceleration voltage was 5.0 kV.

Chemical analyses. Samples were taken from the cultures daily in an anoxic glove box (100% N_2) using a syringe with a needle through the butyl-rubber stopper and centrifuged (14,000 × *g*, 10 min). For quantification of Fe(II) and Fe(III), a revised ferrozine protocol for nitrite-containing samples was used to eliminate the abiotic reaction of nitrite with Fe(II) during acidification (21, 81). The purple ferrozine-Fe(II) complex was quantified at 562 nm using a microtiter plate reader; all ferrozine measurements

were done in triplicate. Nitrate, nitrite, and ammonium samples were diluted with anoxic Milli-Q H_2O and stored under anoxic conditions at 4°C until analysis using a continuous-flow analyzer (flow injection analysis [FIA] system) was done, following standard protocols provided by the instrument manufacturer. The system was equipped with a dialysis membrane for Fe removal to prevent side reactions during analysis (3-Quattro; Bran & Luebbe, Seal Analytical, Norderstedt, Germany). Rates of microbial Fe^{2+} oxidation and nitrate reduction were calculated from the slope between the first and last data point in each of the three Fe(II) oxidation phases specified in detail later in the manuscript.

Mineralogical analysis. X-ray diffraction (XRD) was performed using Bruker's D8 Discover GADDS XRD^2 microdiffractometer equipped with a standard sealed tube with a Co anode (Co Kα radiation, λ = 0.17903 nm) at parameters of 30 kV/30 mA. The total time of measurement was 240 s at two detector positions (15 and 40°). Resulting diffractograms were analyzed using the software Match! (version 3.6.2.121). Phase identification of minerals was performed using Mössbauer spectroscopy. Liquid-suspended mineral precipitates were passed through a filter (0.45 μm, Millipore) and then sealed between two layers of oxygen-impermeable adhesive polyimide film (Kapton) and sealed in a Schott bottle. The sample was inserted into a closed-cycle exchange gas cryostat (Janis cryogenics) with spectra measured at 77 K using a constant acceleration drive system (WissEL) in transmission mode with a ^{57}Co/Rh source and calibrated against a 7-μm-thick α-^{57}Fe foil measured at room temperature. Spectra were analyzed using Recoil (University of Ottawa) by applying the Voigt-based fitting (VBF) routine (82). The half width at half maximum (HWHM) was fixed to a value of 0.125 mm/s for all samples, which was determined to be the inner line broadening of the calibration foil at room temperature.

Phylogenetic analysis. DNA from the enrichment culture was extracted with the FastDNA spin kit for soil (MP Biomedicals) according to the user manual. 16S rRNA gene amplicons were analyzed using PacBio Sequel single-molecule, real-time (SMRT) long-read amplicon sequencing. Two rounds of PCR were applied for DNA amplification. The first PCR was performed using the KAPA HiFi ReadyMix PCR kit (KAPA BioSystems, Cape Town, South Africa) and universal 16S primers tailed with PacBio universal sequencing adapters (universal tags) and 5′ amino modifiers C6 in a first round of PCR (27F gcagtcgaa catgtagctgactcaggtcac [tailed universal sequence], AGRGTTYGATYMTGGCTCAG [primer sequence], 1492R tggatcacttgtgcaagcatcacatcgtag, RGYTACCTTGTTACGACTT) (Eurofins Genomics, Ebersberg, Germany). The following PCR program was used for the first PCR with 26 cycles: initial denaturation for 3 min at 95°C, denaturation for 30 s at 95°C, annealing for 30 s at 57°C, and extension for 60 s at 72°C. Amplicons were purified with the QIAquick PCR purification kit (Qiagen, Hilden, Germany) according to the user manual. The second PCR was performed using the KAPA HiFi ReadyMix PCR kit and PacBio Barcoded Universal F/R Primers Plate, 96 (Pacific Biosciences, CA, USA), followed by AMPure PB bead kit (PacBio biosciences, CA, USA) purification according to the user manual. The following PCR program was used for the second PCR with 20 cycles: denaturation for 30 s at 95°C, annealing for 30 s at 57°C, and extension for 60 s at 72°C. The quality and quantity of PCR products were checked by an Agilent 2100 bioanalyzer system (Agilent, CA, USA) after each PCR. SMRTbell library preparation and further purification were achieved by SMRTbell Template Prep kit (PacBio biosciences, CA, USA) and by following the user instructions.

Circular consensus sequencing reads were analyzed with DADA2 version 1.10.0 (83) in R version 3.5.1 (79) by sequentially orienting reads and removing primers, filtering (no ambiguous nucleotides and maximum 2 expected errors) and trimming (1,000 bp to 1,600 bp read length), dereplicating sequences, learning error rates, removing bimera *de novo*, and finally assigning taxonomy to the detected sequences based on SILVA version 132 (84). Results are discussed in the manuscript as relative bacterial 16S rRNA gene sequence abundance of ASVs as a proportion of the total number of reads per sample.

For constructing a phylogenetic tree, selected full-length 16S rRNA gene sequences (minimum length 1,460 bp) from close relatives of dominant bacteria in the culture, as well as more distantly related known potential NRFeOx bacteria, were downloaded from the NCBI database. Bacterial 16S rRNA gene sequence from *Mariprofundus ferrooxydans* PV-1, a microaerophilic Fe(II) oxidizer belonging to the novel *Zetaproteobacteria* class, was chosen as an outgroup. MUSCLE implemented in the MEGA X software (85) was used for alignment of the 16S rRNA gene sequences with default parameters. A consensus neighbor-joining tree of the most abundant taxa from the enrichment culture was constructed in MEGA X using the maximum-likelihood method with 1,000 bootstrap replicates.

Data availability. Raw sequencing data have been deposited at DDBJ/ENA/GenBank under BioProject accession number PRJNA592904.

SUPPLEMENTAL MATERIAL

Supplemental material is available online only.

SUPPLEMENTAL FILE 1, PDF file, 1 MB.

ACKNOWLEDGMENTS

This work is supported by the Collaborative Research Center 1253 CAMPOS (project 5: fractured aquifer and p2: sub-catchments), funded by the German Research Foundation (DFG, Grant Agreement SFB 1253/1). Daniel Straub is funded by the Institutional Strategy of the University of Tübingen (DFG, ZUK63). Sara Kleindienst is funded by an Emmy Noether grant (grant number 326028733) from the DFG. The authors acknowledge support by the state of Baden-Württemberg through bwHPC and

the German Research Foundation (DFG) through grant number INST 37/935-1 FUGG (bwForCluster BinAC). A.K. acknowledges infrastructural support by the DFG under Germany's Excellence Strategy, cluster of Excellence EXC2124, project ID 390838134.

We thank Ellen Röhm for nitrate and nitrite analyses, André Pellerin for AVS measurements, Anna-Neva Visser for the development of Microbial Trapping Devices (MTDs), and Franziska Schädler for help with DNA extractions.

REFERENCES

1. Ward MH, Jones RR, Brender JD, de Kok TM, Weyer PJ, Nolan BT, Villanueva CM, van Breda SG. 2018. Drinking water nitrate and human health: an updated review. Int J Environ Res Public Health 15:1–31. https://doi.org/10.3390/ijerph15071557.
2. World Health Organization. 2011. Guidelines for drinking-water quality, fourth edition.
3. Kim H, Kaown D, Mayer B, Lee J-Y, Hyun Y, Lee K-K. 2015. Identifying the sources of nitrate contamination of groundwater in an agricultural area (Haean basin, Korea) using isotope and microbial community analyses. Sci Total Environ 533:566–575. https://doi.org/10.1016/j.scitotenv.2015.06.080.
4. Opazo T, Aravena R, Parker B. 2016. Nitrate distribution and potential attenuation mechanisms of a municipal water supply bedrock aquifer. Appl Geochem 73:157–168. https://doi.org/10.1016/j.apgeochem.2016.08.010.
5. Wick K, Heumesser C, Schmid E. 2012. Groundwater nitrate contamination: factors and indicators. J Environ Manage 111:178–186. https://doi.org/10.1016/j.jenvman.2012.06.030.
6. Rezvani F, Sarrafzadeh M-H, Ebrahimi S, Oh H-M. 2019. Nitrate removal from drinking water with a focus on biological methods: a review. Environ Sci Pollut Res Int 26:1124–1141. https://doi.org/10.1007/s11356-017-9185-0.
7. Jensen VB, Darby JL, Seidel C, Gorman C. 2014. Nitrate in potable water supplies: alternative management strategies. Crit Rev Environ Sci Technol 44:2203–2286. https://doi.org/10.1080/10643389.2013.828272.
8. Robertson EK, Thamdrup B. 2017. The fate of nitrogen is linked to iron(II) availability in a freshwater lake sediment. Geochim Cosmochim Acta 205:84–99. https://doi.org/10.1016/j.gca.2017.02.014.
9. van den Berg EM, Rombouts JL, Kuenen JG, Kleerebezem R, van Loosdrecht MCM. 2017. Role of nitrite in the competition between denitrification and DNRA in a chemostat enrichment culture. AMB Express 7:91–97. https://doi.org/10.1186/s13568-017-0398-x.
10. Burgin AJ, Hamilton SK. 2007. Have we overemphasized the role of denitrification in aquatic ecosystems? A review of nitrate removal pathways. Front Ecol Environ 5:89–96. https://doi.org/10.1890/1540-9295(2007)5[89:HWOTRO]2.0.CO;2.
11. Tiedje JM. 1988. Ecology of denitrification and dissimilatory nitrate reduction to ammonium, p 179–244. *In* Zehnder AJB (ed), Biology of anaerobic microorganisms. John Wiley and Sons, New York, NY.
12. Rivett MO, Buss SR, Morgan P, Smith JWN, Bemment CD. 2008. Nitrate attenuation in groundwater: a review of biogeochemical controlling processes. Water Res 42:4215–4232. https://doi.org/10.1016/j.watres.2008.07.020.
13. Herrmann M, Opitz S, Harzer R, Totsche KU, Küsel K. 2017. Attached and suspended denitrifier communities in pristine limestone aquifers harbor high fractions of potential autotrophs oxidizing reduced iron and sulfur compounds. Microb Ecol 74:264–277. https://doi.org/10.1007/s00248-017-0950-x.
14. Kumar S, Herrmann M, Blohm A, Hilke I, Frosch T, Trumbore SE, Küsel K. 2018. Thiosulfate- and hydrogen-driven autotrophic denitrification by a microbial consortium enriched from groundwater of an oligotrophic limestone aquifer. FEMS Microbiol Ecol 94:fiy141. https://doi.org/10.1093/femsec/fiy141.
15. Di Capua F, Pirozzi F, Lens PNL, Esposito G. 2019. Electron donors for autotrophic denitrification. Chem Eng J 362:922–937. https://doi.org/10.1016/j.cej.2019.01.069.
16. Benz M, Brune A, Schink B. 1998. Anaerobic and aerobic oxidation of ferrous iron at neutral pH by chemoheterotrophic nitrate-reducing bacteria. Arch Microbiol 169:159–165. https://doi.org/10.1007/s002030050555.
17. Kappler A, Schink B, Newman K. 2005. Fe(III) mineral formation and cell encrustation by the nitrate-dependent Fe(II)-oxidizer strain BoFeN1. Geobiology 3:235–245. https://doi.org/10.1111/j.1472-4669.2006.00056.x.
18. Liu T, Chen D, Li X, Li F. 2019. Microbially mediated coupling of nitrate reduction and Fe(II) oxidation under anoxic conditions. FEMS Microbiol Ecol 95:fiz030. https://doi.org/10.1093/femsec/fiz030.
19. Muehe EM, Gerhardt S, Schink B, Kappler A. 2009. Ecophysiology and the energetic benefit of mixotrophic Fe(II) oxidation by various strains of nitrate-reducing bacteria. FEMS Microbiol Ecol 70:335–343. https://doi.org/10.1111/j.1574-6941.2009.00755.x.
20. Bryce C, Blackwell N, Schmidt C, Otte J, Huang Y-M, Kleindienst S, Tomaszewski E, Schad M, Warter V, Peng C, Byrne JM, Kappler A. 2018. Microbial anaerobic Fe(II) oxidation - ecology, mechanisms and environmental implications. Environ Microbiol 20:3462–3483. https://doi.org/10.1111/1462-2920.14328.
21. Klueglein N, Kappler A. 2013. Abiotic oxidation of Fe(II) by reactive nitrogen species in cultures of the nitrate-reducing Fe(II) oxidizer *Acidovorax* sp. BoFeN1 – questioning the existence of enzymatic Fe(II) oxidation. Geobiology 11:180–190. https://doi.org/10.1111/gbi.12019.
22. Nordhoff M, Tominski C, Halama M, Byrne JM, Obst M, Kleindienst S, Behrens S, Kappler A. 2017. Insights into nitrate-reducing Fe(II) oxidation mechanisms through analysis of cell-mineral associations, cell encrustation, and mineralogy in the chemolithoautotrophic enrichment culture KS. Appl Environ Microbiol 83:e00752-17. https://doi.org/10.1128/AEM.00752-17.
23. Kappler A, Bryce C, Mansor M, Lueder U, Byrne JM, Swanner ED. 2021. An evolving view on biogeochemical cycling of iron. Nat Rev Microbiol 19:360–374. https://doi.org/10.1038/s41579-020-00502-7.
24. Straub KL, Benz M, Schink B, Widdel E. 1996. Anaerobic, nitrate-dependent microbial oxidation of ferrous iron. Appl Environ Microbiol 62:1458–1460. https://doi.org/10.1128/aem.62.4.1458-1460.1996.
25. Blöthe M, Roden EE. 2009. Composition and activity of an autotrophic Fe (II)-oxidizing, nitrate-reducing enrichment culture. Appl Environ Microbiol 75:6937–6940. https://doi.org/10.1128/AEM.01742-09.
26. Tominski C, Heyer H, Lösekann-Behrens T, Behrens S, Kappler A. 2018. Growth and population dynamics of the anaerobic Fe(II)-oxidizing and nitrate-reducing enrichment culture KS. Appl Environ Microbiol 84:e02173-17. https://doi.org/10.1128/AEM.02173-17.
27. Beller HR. 2005. Anaerobic, nitrate-dependent oxidation of U (IV) oxide minerals by the chemolithoautotrophic bacterium *Thiobacillus denitrificans*. Appl Environ Microbiol 71:2170–2174. https://doi.org/10.1128/AEM.71.4.2170-2174.2005.
28. Weber KA, Picardal FW, Roden EE. 2001. Microbially catalyzed nitrate-dependent oxidation of biogenic solid-phase Fe(II) compounds. Environ Sci Technol 35:1644–1650. https://doi.org/10.1021/es0016598.
29. Herndon E, Albashaireh A, Singer D, Roy T, Gu B, Graham D, Hall M. 2017. Influence of iron redox cycling on organo-mineral associations in Arctic tundra soil. Geochim Cosmochim Acta 207:210–231. https://doi.org/10.1016/j.gca.2017.02.034.
30. Jørgensen CJ, Jacobsen OS, Elberling B, Aamand J. 2009. Microbial oxidation of pyrite coupled to nitrate reduction in anoxic groundwater sediment. Environ Sci Technol 43:4851–4857. https://doi.org/10.1021/es803417s.
31. Herrmann M, Rusznyák A, Akob DM, Schulze I, Opitz S, Totsche KU, Küsel K. 2015. Large fractions of CO_2-fixing microorganisms in pristine limestone aquifers appear to be involved in the oxidation of reduced sulfur and nitrogen compounds. Appl Environ Microbiol 81:2384–2394. https://doi.org/10.1128/AEM.03269-14.
32. Rimstidt DD, Vaughan DJ. 2003. Pyrite oxidation: a state-of-the-art assessment of the reaction mechanism. Geochim Cosmochim Acta 67:873–880. https://doi.org/10.1016/S0016-7037(02)01165-1.
33. Percak-Dennett E, He S, Converse B, Konishi H, Xu H, Corcoran A, Noguera D, Chan C, Bhattacharyya A, Borch T, Boyd E, Roden EE. 2017. Microbial acceleration of aerobic pyrite oxidation at circumneutral pH. Geobiology 15:690–703. https://doi.org/10.1111/gbi.12241.
34. Bosch J, Lee KY, Jordan G, Kim KW, Meckenstock RU. 2012. Anaerobic, nitrate-dependent oxidation of pyrite nanoparticles by *Thiobacillus denitrificans*. Environ Sci Technol 46:2095–2101. https://doi.org/10.1021/es2022329.

35. Vaclavkova S, Schultz-Jensen N, Jacobsen OS, Elberling B, Aamand J. 2015. Nitrate-controlled anaerobic oxidation of pyrite by *Thiobacillus* cultures. Geomicrobiol J 32:412–419. https://doi.org/10.1080/01490451.2014.940633.
36. Torrentó C, Urmeneta J, Otero N, Soler A, Viñas M, Cama J. 2011. Enhanced denitrification in groundwater and sediments from a nitrate-contaminated aquifer after addition of pyrite. Chem Geol 287:90–101. https://doi.org/10.1016/j.chemgeo.2011.06.002.
37. Haaijer SCM, Lamers LPM, Smolders AJP, Jetten MSM, Op de Camp HJM. 2007. Iron sulfide and pyrite as potential electron donors for microbial nitrate reduction in freshwater wetlands. Geomicrobiol J 24:391–401. https://doi.org/10.1080/01490450701436489.
38. Peiffer S, Stubert I. 1999. The oxidation of pyrite at pH 7 in the presence of reducing and nonreducing Fe(III)-chelators. Geochim Cosmochim Acta 63:3171–3182. https://doi.org/10.1016/S0016-7037(99)00224-0.
39. Pauwels H. 1994. Natural denitrification in groundwater in the presence of pyrite: preliminary results obtained at Naizin (Brittany, France). Mineral Mag 58A:696–697. https://doi.org/10.1180/minmag.1994.58A.2.100.
40. Pauwels H, Kloppmann W, Foucher JC, Martelat A, Fritsche V. 1998. Field tracer test for denitrification in a pyrite-bearing schist aquifer. Appl Geochemistry 13:767–778. https://doi.org/10.1016/S0883-2927(98)00003-1.
41. Jewell TNM, Karaoz U, Brodie EL, Williams KH, Beller HR. 2016. Metatranscriptomic evidence of pervasive and diverse chemolithoautotrophy relevant to C, S, N and Fe cycling in a shallow alluvial aquifer. ISME J 10:2106–2117. https://doi.org/10.1038/ismej.2016.25.
42. Torrentó C, Cama J, Urmeneta J, Otero N, Soler A. 2010. Denitrification of groundwater with pyrite and *Thiobacillus denitrificans*. Chem Geol 278:80–91. https://doi.org/10.1016/j.chemgeo.2010.09.003.
43. Schwientek M, Einsiedl F, Stichler W, Stögbauer A, Strauss H, Maloszewski P. 2008. Evidence for denitrification regulated by pyrite oxidation in a heterogeneous porous groundwater system. Chem Geol 255:60–67. https://doi.org/10.1016/j.chemgeo.2008.06.005.
44. Zhang Y-C, Slomp CP, Broers HP, Bostick B, Passier HF, Böttcher ME, Omoregie EO, Lloyd JR, Polya DA, Van Cappellen P. 2012. Isotopic and microbiological signatures of pyrite-driven denitrification in a sandy aquifer. Chem Geol 300–301:123–132. https://doi.org/10.1016/j.chemgeo.2012.01.024.
45. Postma D, Boesen C, Kristiansen H, Larsen F. 1991. Nitrate reduction in an unconfined sandy aquifer: water chemistry, reduction processes, and geochemical modeling. Water Resour Res 27:2027–2045. https://doi.org/10.1029/91WR00989.
46. Huang Y-M, Straub D, Kappler A, Smith N, Blackwell N, Kleindienst S. 2021. A novel enrichment culture highlights core features of microbial networks contributing to autotrophic Fe(II) oxidation coupled to nitrate reduction. Microb Physiol, in press. https://doi.org/10.1159/000517083.
47. Emerson D, Field EK, Chertkov O, Davenport KW, Goodwin L, Munk C, Nolan M, Woyke T. 2013. Comparative genomics of freshwater Fe-oxidizing bacteria: implications for physiology, ecology, and systematics. Front Microbiol 4:254. https://doi.org/10.3389/fmicb.2013.00254.
48. He S, Barco RA, Emerson D, Roden EE. 2017. Comparative genomic analysis of neutrophilic iron(II) oxidizer genomes for candidate genes in extracellular electron transfer. Front Microbiol 8:1584. https://doi.org/10.3389/fmicb.2017.01584.
49. He S, Tominski C, Kappler A, Behrens S, Roden EE. 2016. Metagenomic analyses of the autotrophic Fe(II)-oxidizing, nitrate-reducing enrichment culture KS. Appl Environ Microbiol 82:2656–2668. https://doi.org/10.1128/AEM.03493-15.
50. Carlson HK, Clark IC, Blazewicz SJ, Iavarone AT, Coates JD. 2013. Fe(II) oxidation is an innate capability of nitrate-reducing bacteria that involves abiotic and biotic reactions. J Bacteriol 195:3260–3268. https://doi.org/10.1128/JB.00058-13.
51. Chakraborty A, Roden EE, Schieber J, Picardal F. 2011. Enhanced growth of *Acidovorax* sp. strain 2AN during nitrate-dependent Fe(II) oxidation in batch and continuous-flow systems. Appl Environ Microbiol 77:8548–8556. https://doi.org/10.1128/AEM.06214-11.
52. Zhang T, Shao MF, Ye L. 2012. 454 pyrosequencing reveals bacterial diversity of activated sludge from 14 sewage treatment plants. ISME J 6:1137–1147. https://doi.org/10.1038/ismej.2011.188.
53. Chourey K, Nissen S, Vishnivetskaya T, Shah M, Pfiffner S, Hettich RL, Löffler FE. 2013. Environmental proteomics reveals early microbial community responses to biostimulation at a uranium- and nitrate-contaminated site. Proteomics 13:2921–2930. https://doi.org/10.1002/pmic.201300155.
54. Mcilroy SJ, Starnawska A, Starnawski P, Saunders AM, Nierychlo M, Nielsen PH, Nielsen JL. 2016. Identification of active denitrifiers in full-scale nutrient removal wastewater treatment systems. Environ Microbiol 18:50–64. https://doi.org/10.1111/1462-2920.12614.
55. Chakraborty A, Picardal F. 2013. Neutrophilic, nitrate-dependent, Fe(II) oxidation by a *Dechloromonas* species. World J Microbiol Biotechnol 29:617–623. https://doi.org/10.1007/s11274-012-1217-9.
56. Polcyn W, Luciński R. 2003. Aerobic and anaerobic nitrate and nitrite reduction in free-living cells of *Bradyrhizobium* sp. (*Lupinus*). FEMS Microbiol Lett 226:331–337. https://doi.org/10.1016/S0378-1097(03)00620-7.
57. Siqueira AF, Minamisawa K, Sánchez C. 2017. Anaerobic reduction of nitrate to nitrous oxide is lower in Bradyrhizobium japonicum than in Bradyrhizobium diazoefficiens. Microbes Environ 32:398–401. https://doi.org/10.1264/jsme2.ME17081.
58. Coates JD, Ellis DJ, Gaw CV, Lovley DR. 1999. *Geothrix fermentans* gen. nov., sp. nov., a novel Fe(III)-reducing bacterium from a hydrocarbon-contaminated aquifer. Int J Syst Evol Microbiol 49:1614–1622. https://doi.org/10.1099/00207713-49-4-1615.
59. Guerbois D, Ona-Nguema G, Morin G, Abdelmoula M, Laverman AM, Mouchel JM, Barthelemy K, Maillot F, Brest J. 2014. Nitrite reduction by biogenic hydroxycarbonate green rusts: evidence for hydroxy-nitrite green rust formation as an intermediate reaction product. Environ Sci Technol 48:4505–4514. https://doi.org/10.1021/es404009k.
60. Bollag J-M, Henninger NM. 1978. Effects of nitrite toxicity on soil bacteria aerobic and anaerobic. Soil Biol Biochem 10:377–381. https://doi.org/10.1016/0038-0717(78)90061-5.
61. Weber KA, Pollock J, Cole KA, Connor SMO, Achenbach LA, Coates JD. 2006. Anaerobic nitrate-dependent iron(II) bio-oxidation by a novel lithoautotrophic Betaproteobacterium, strain 2002. Appl Environ Microbiol 72:686–694. https://doi.org/10.1128/AEM.72.1.686-694.2006.
62. Chen D, Liu T, Li X, Li F, Luo X, Wu Y, Wang Y. 2018. Biological and chemical processes of microbially mediated nitrate-reducing Fe(II) oxidation by *Pseudogulbenkiania* sp. strain 2002. Chem Geol 476:59–69. https://doi.org/10.1016/j.chemgeo.2017.11.004.
63. Buresh RJ, Moraghan JT. 1976. Chemical reduction of nitrate by ferrous iron. J Environ Qual 5:320–325. https://doi.org/10.2134/jeq1976.00472425000500030021x.
64. Van Cleemput O, Baert L. 1983. Nitrite stability influenced by iron compounds. Soil Biol Biochem 15:137–140. https://doi.org/10.1016/0038-0717(83)90093-7.
65. Rakshit S, Matocha CJ, Coyne MS. 2008. Nitrite reduction by siderite. Soil Sci Soc Am J 72:1070–1077. https://doi.org/10.2136/sssaj2007.0296.
66. Visser AN, Wankel SD, Niklaus PA, Byrne JM, Kappler AA, Lehmann MF. 2020. Impact of reactive surfaces on the abiotic reaction between nitrite and ferrous iron and associated nitrogen and oxygen isotope dynamics. Biogeosciences 17:4355–4374. https://doi.org/10.5194/bg-17-4355-2020.
67. Laufer K, Røy H, Jørgensen BB, Kappler A. 2016. Evidence for the existence of autotrophic nitrate-reducing Fe(II)-oxidizing bacteria in marine coastal sediment. Appl Environ Microbiol 82:6120–6131. https://doi.org/10.1128/AEM.01570-16.
68. Eickhoff M, Obst M, Schro C, Hitchcock AP, Tyliszczak T, Martinez RE, Robbins LJ, Konhauser KO, Kappler A. 2014. Nickel partitioning in biogenic and abiogenic ferrihydrite: the influence of silica and implications for ancient environments. Geochim Cosmochim Acta 140:65–79. https://doi.org/10.1016/j.gca.2014.05.021.
69. Hegler F, Posth NR, Jiang J, Kappler A. 2008. Physiology of phototrophic iron(II)-oxidizing bacteria: implications for modern and ancient environments. FEMS Microbiol Ecol 66:250–260. https://doi.org/10.1111/j.1574-6941.2008.00592.x.
70. Sobolev D, Roden EE. 2004. Characterization of a neutrophilic, chemolithoautotrophic Fe(II)-oxidizing β-proteobacterium from freshwater wetland sediments. Geomicrobiol J 21:1–10. https://doi.org/10.1080/01490450490253310.
71. Kappler A, Newman DK. 2004. Formation of Fe(III)-minerals by Fe(II)-oxidizing photoautotrophic bacteria. Geochim Cosmochim Acta 68:1217–1226. https://doi.org/10.1016/j.gca.2003.09.006.
72. Shi L, Dong H, Reguera G, Beyenal H, Lu A, Liu J, Yu HQ, Fredrickson JK. 2016. Extracellular electron transfer mechanisms between microorganisms and minerals. Nat Rev Microbiol 14:651–662. https://doi.org/10.1038/nrmicro.2016.93.
73. Visser AN, Lehmann MF, Rügner H, D'Affonseca FM, Grathwohl P, Blackwell N, Kappler A, Osenbrück K. 2021. Fate of nitrate during groundwater recharge in a fractured karst aquifer in Southwest Germany. Hydrogeol J 29:1153–1171. https://doi.org/10.1007/s10040-021-02314-2.
74. Griebler C, Mindl B, Slezak D, Geiger-Kaiser M. 2002. Distribution patterns of attached and suspended bacteria in pristine and contaminated shallow aquifers studied with an in situ sediment exposure microcosm. Aquat Microb Ecol 28:117–129. https://doi.org/10.3354/ame028117.
75. Küsel K, Totsche KU, Trumbore SE, Lehmann R, Steinhäuser C, Herrmann M. 2016. How deep can surface signals be traced in the critical zone?

Merging biodiversity with biogeochemistry research in a central German Muschelkalk landscape. Front Earth Sci 4:32. https://doi.org/10.3389/feart.2016.00032.
76. Widdel F. 1980. Anaerober Abbau von Fettsäuren und Benzoesäure durch neu isolierte Arten. Diss Thesis, Univ Göttingen.
77. Burke KA, Calder K, Lascelles J. 1980. Effects of molybdenum and tungsten on induction of nitrate reductase and formate dehydrogenase in wild type and mutant *Paracoccus denitrificans*. Arch Microbiol 126:155–159. https://doi.org/10.1007/BF00511221.
78. Kappler A, Johnson CM, Crosby HA, Beard BL, Newman DK. 2010. Evidence for equilibrium iron isotope fractionation by nitrate-reducing iron (II)-oxidizing bacteria. Geochim Cosmochim Acta 74:2826–2842. https://doi.org/10.1016/j.gca.2010.02.017.
79. R Core Team. 2018. R: a language and environment for statistical computing. R Foundation for Statistical Computing, Vienna, Austria.
80. Zeitvogel F, Burkhardt CJ, Schroeppel B, Schmid G, Ingino P, Obst M. 2017. Comparison of preparation methods of bacterial cell-mineral aggregates for SEM imaging and analysis using the model system of *Acidovorax* sp. Geomicrobiol J 34:317–327. https://doi.org/10.1080/01490451.2016.1189467.
81. Schaedler F, Kappler A, Schmidt C. 2018. A revised iron extraction protocol for environmental samples rich in nitrite and carbonate. Geomicrobiol J 35:23–30. https://doi.org/10.1080/01490451.2017.1303554.
82. Rancourt DG, Ping JY. 1991. Voigt-based distributions methods for arbitrary-shape in Mössbauer spectroscopy static hyperfine parameter. Nucl Instruments Methods Phys Res 58:85–97. https://doi.org/10.1016/0168-583X(91)95681-3.
83. Callahan BJ, Wong J, Heiner C, Oh S, Theriot CM, Gulati S, Mcgill SK, Dougherty MK. 2019. High-throughput amplicon sequencing of the full-length 16S rRNA gene with single-nucleotide resolution. Nucleic Acids Res 47:e103. https://doi.org/10.1093/nar/gkz569.
84. Callahan BJ. 2018. Silva taxonomic training data formatted for DADA2 (Silva version 132) [Data set]. Zenodo, CERN, Geneva, Switzerland. https://doi.org/10.5281/zenodo.1172783.
85. Kumar S, Stecher G, Li M, Knyaz C, Tamura K. 2018. MEGA X: molecular evolutionary genetics analysis across computing platforms. Mol Biol Evol 35:1547–1549. https://doi.org/10.1093/molbev/msy096.
86. Pruesse E, Peplies J, Glöckner FO. 2012. SINA: accurate high-throughput multiple sequence alignment of ribosomal RNA genes. Bioinformatics 28:1823–1829. https://doi.org/10.1093/bioinformatics/bts252.